Published OnlineFirst October 19, 2016; DOI: 10.1158/1078-0432.CCR-16-1317

Cancer Therapy: Preclinical

Clinical Cancer Research

Inhibition of *STAT3* with the Generation 2.5 Antisense Oligonucleotide, AZD9150, Decreases Neuroblastoma Tumorigenicity and Increases Chemosensitivity

Seiichi Odate[1], Veronica Veschi[1], Shuang Yan[1], Norris Lam[1], Richard Woessner[2], and Carol J. Thiele[1]

Abstract

Purpose: Neuroblastoma is a pediatric tumor of peripheral sympathoadrenal neuroblasts. The long-term event-free survival of children with high-risk neuroblastoma is still poor despite the improvements with current multimodality treatment protocols. Activated JAK/STAT3 pathway plays an important role in many human cancers, suggesting that targeting STAT3 is a promising strategy for treating high-risk neuroblastoma.

Experimental Design: To evaluate the biologic consequences of specific targeting of STAT3 in neuroblastoma, we assessed the effect of tetracycline (Tet)-inducible STAT3 shRNA and the generation 2.5 antisense oligonucleotide AZD9150 which targets STAT3 in three representative neuroblastoma cell line models (AS, NGP, and IMR32).

Results: Our data indicated that Tet-inducible STAT3 shRNA and AZD9150 inhibited endogenous STAT3 and STAT3 target genes. Tet-inducible STAT3 shRNA and AZD9150 decreased cell growth and tumorigenicity. *In vivo*, STAT3 inhibition by Tet-inducible STAT3 shRNA or AZD9150 alone had little effect on growth of established tumors. However, when treated xenograft tumor cells were reimplanted into mice, there was a significant decrease in secondary tumors in the mice receiving AZD9150-treated tumor cells compared with the mice receiving ntASO-treated tumor cells. This indicates that inhibition of STAT3 decreases the tumor-initiating potential of neuroblastoma cells. Furthermore, inhibition of STAT3 significantly increased neuroblastoma cell sensitivity to cisplatin and decreased tumor growth and increased the survival of tumor-bearing mice *in vivo*.

Conclusions: Our study supports the development of strategies targeting STAT3 inhibition in combination with conventional chemotherapy for patients with high-risk neuroblastoma. *Clin Cancer Res; 23(7); 1771–84. ©2016 AACR.*

Introduction

Neuroblastoma is the most common extracranial solid tumor in childhood and arises from the embryonic neural crest (1). It accounts for almost 8% of pediatric malignancies and causes 10% of all pediatric oncology deaths (2). Patients with localized, low- and intermediate-risk neuroblastoma are mostly curable and have excellent long-term survival rates with standard therapies. In contrast, patients with high-risk aggressive neuroblastoma have a dismal outcome. Despite the current intensive therapy such as intensive chemotherapy, radiotherapy, and bone marrow transplantation, the long-term event-free survival rate of these patients is less than 50% (3). Therefore, more effective treatment strategies are urgently needed for patients with high-risk neuroblastoma.

Targeting mutant or dysregulated signal transduction pathways in malignant tumors is a promising approach to improve therapies. Aberrant activation of JAK/STAT3 signaling, in particular STAT3, participates in the initiation, development, and progression of human cancer (4, 5). JAK/STAT3 pathway transduces signals from cytokines, interleukins, and growth factors, such as IL6 and G-CSF (6). A number of STAT3 downstream transcriptional targets encode antiapoptotic proteins, cell-cycle regulators, and angiogenic factors such as Bcl-2, cyclin D1, and VEGF (7) that are dysregulated in cancers. Previous findings have shown that the aberrant activation of JAK/STAT3 pathway participates in a wide variety of malignancies, including hematopoietic malignancies (leukemia, lymphoma, and multiple myeloma) as well as solid tumors (such as head and neck, breast, lung, prostate, renal, and rectal cancers; refs. 8–17). Activation of the STAT3 pathway has been found to be important for maintenance of a cancer stem cell–like subpopulation in several malignancies such as bladder cancer, colon cancer, hepatocellular carcinoma, and malignant gliomas (18–21).

An involvement of STAT3 in neuroblastoma tumor biology was first identified when elevated levels of IL6 in the bone marrow and peripheral blood were linked to poor prognosis in high-risk patients (22, 23). In preclinical models, *in vitro* studies also showed that bone marrow–derived IL6 increased the proliferation and decreased cytotoxic drug–induced apoptosis via STAT3 activation in neuroblastoma cells (23). More recent findings implicated STAT3 as a critical mediator of a subpopulation of

[1]Cell & Molecular Biology Section, Pediatric Oncology Branch, Center for Cancer Research, National Cancer Institute, Bethesda, Maryland. [2]Cancer Bioscience Drug Discovery, AstraZeneca Pharmaceuticals, Waltham, Massachusetts.

Note: Supplementary data for this article are available at Clinical Cancer Research Online (http://clincancerres.aacrjournals.org/).

Corresponding Author: Carol J. Thiele, Cell & Molecular Biology Section, Pediatric Oncology Branch, Center for Cancer Research, National Cancer Institute, Bethesda, MD 20892. Phone: 301-496-1543; Fax: 301-451-7052; E-mail: thielec@mail.nih.gov

doi: 10.1158/1078-0432.CCR-16-1317

Published OnlineFirst October 19, 2016; DOI: 10.1158/1078-0432.CCR-16-1317

Translational Relevance

This report is the first pediatric preclinical study of the efficacy of AZD9150 in targeting STAT3 in neuroblastoma tumors. Our findings that AZD9150 increases the sensitivity of neuroblastoma cells to cisplatin and decreases neuroblastoma tumorigenicity suggest future clinical evaluation of selective STAT3 inhibition in combination with conventional cytotoxic therapy for patients with high-risk neuroblastoma. Such a strategy may increase therapeutic effectiveness and decrease morbidities associated with conventional chemotherapy.

neuroblastoma cells with increased tumorigenicity and metastatic capabilities (24). These cells also express G-CSF receptor (G-CSFR/CD114) and blocking the G-CSF/STAT3 signaling axis with either an anti–G-CSF antibody or with Stattic, a small-molecule inhibitor of STAT3, reverses the protumorigenic effects after G-CSF (24, 25). Given that drug-resistant metastasis and recurrence are common causes of relapse in patients with high-risk neuroblastoma (26), STAT3 may be a promising molecular target for high-risk neuroblastoma.

We first reported that AZD1480, an ATP competitive inhibitor of JAK1 and JAK2, inactivated STAT3-mediated signaling and inhibited tumor growth in pediatric solid tumors such as neuroblastoma, Ewing sarcoma, and rhabdomyosarcoma *in vitro* and *in vivo* (27). Given the activity spectrum of AZD1480 against a number of different kinases, we sought to evaluate how specific inhibition of endogenous STAT3 affects neuroblastoma cell growth as well as their sensitivity to cytotoxic agents. We evaluated the antitumor growth effect of specific inhibition of STAT3 alone and in combination with cisplatin *in vitro* and *in vivo* using specific genetic knockdown and a first-in-class generation 2.5 antisense oligonucleotide (ASO) targeting STAT3, AZD9150 (28) which has shown activity in a phase I study of highly treatment refractory lymphoma (28). This study is the first preclinical study to evaluate AZD9150 in a pediatric cancer. Furthermore, it shows that genetic inhibition using shSTAT3 or pharmacologic inhibition using AZD9150 inhibits STAT3 expression and activation of downstream STAT3 targets and leads to decreases in neuroblastoma cell tumor-initiating potential and increases chemosensitivity.

Materials and Methods

Cell lines and reagents

Human neuroblastoma cell lines (SK-N-AS, NGP, IMR32) are from NCI/POB stocks in the laboratory of C.J. Thiele and were maintained as previously detailed (29). These cell lines have been determined to be genetically pure using an SNP-based genotype assay (kindly performed by S.J. Chanock, Division of Cancer Genetics and Epidemiology, NCI, Bethesda, MD). Tetracycline (Tet)-inducible shRNA targeting human STAT3 and vector control shRNAs were purchased from Clontech Laboratories. Cells were prepared by lentiviral infection of 3 different Tet-inducible shRNA targeting STAT3 (clone ID: V3THS_376016, clone ID _376017, and clone ID _262105) into 3 separate cultures of SK-N-AS, NGP and IMR32 neuroblastoma cell lines and selected with puromycin (0.5 μg/mL for NGP and IMR32 and 1.0 μg/mL for AS). Antibiotic-resistant transfectants were isolated and evaluated for Tet (1 μg/mL)-regulated silencing of human STAT3 mRNA. ASshSTAT3-376017 (ASshSTAT3), NGPshSTAT3-376016 (NGPshSTAT3), and IMR32shSTAT3-376016 (IMR32shSTAT3) were chosen for further study. Comparisons of our standard FBS (Atlanta Biologics S11150 screened to maintain the growth and differentiation potential of neuroblastoma cells) and Clontech Tet-free FBS showed no significant difference in the levels of STAT3mRNA (data not shown), so all *in vitro* experiments were performed with our standard FBS.

AZD9150 (antisense STAT3 oligonucleotide) and a nontargeting antisense oligonucleotide (ntASO) that has the same length, backbone, and base modifications as AZD9150 were provided by AstraZeneca and Ionis Pharmaceuticals. AZD9150 targets nucleotide sequences found only in the human STAT3 gene and these sequences are not present in the murine STAT3 gene (28). For *in vitro* studies, AZD9150 and ntASO were dissolved as a 4.3 and 4.6 mmol/L stock solution, respectively, and frozen in aliquots at −20°C. For *in vivo* experiments, AZD9150 and ntASO were formulated in water, stored at 4°C, and freshly made every week.

Antibodies against phosphorylated STAT3 (Y705, S727), STAT3, cyclin D1, cyclin D3, Bcl-2, survivin, and GAPDH were purchased from Santa Cruz. Antibodies against N-myc, c-myc, phosphorylated ATM (S1981), ATM, phosphorylated Chk2 (T68), Chk2, phosphorylated ATR (S428), ATR, phosphorylated Chk1 (S345), Chk1, γH2AX, and H2AX were purchased from Cell Signaling Technologies.

Cell growth and soft agar assays

To assess the effect of STAT3 on neuroblastoma cell proliferation, neuroblastoma cells and stable clones were plated in triplicate at 1,000 (AS), 3,000 (NGP), or 8,000 (IMR32) cells per well in 96-well plates. The next day, neuroblastoma cells were treated with ntASO (1 μmol/L) or AZD9150 (1 μmol/L), and neuroblastoma cell lines expressing Tet-inducible STAT3 shRNA were treated with or without Tet (1 μg/mL). Cells were cultured in an IncuCyte (Essen Bioscience) and cell confluence was measured every 6 hours.

To assess combination STAT3 inhibition and cisplatin sensitivity, cells were plated in 96-well plates (3,000 cells per well) in triplicate, incubated overnight and then neuroblastoma cells were treated with AZD9150 (1 μmol/L) or ntASO (1 μmol/L), and stable clones were treated with or without Tet (1 μg/mL). After 3 days, cisplatin was added to culture media and cells were incubated for 3 days. Parallel plates were prepared for cell viability assays using of the MTS assay (Promega) as previously described (27, 29). The absorbance (490 nm) was detected using a Versamax microplate reader (Molecular Devices). Cell viability was normalized to untreated cells. The concentration of half-maximal effective inhibition of viability (IC_{50}) was determined using Prism 6.0 software (GraphPad Software Inc.). Each experiment was done in triplicate and results were averaged.

To assess effects of STAT3 inhibition on tumorigenicity, 5,000 cells were cultured in 0.5% top agarose in media containing ntASO (1 μmol/L) or AZD9150 (1 μmol/L) for neuroblastoma cells and containing Tet (1 μg/mL) or not for genetically modified shRNA-expressing cell lines. The top agarose was plated on a layer of 1% bottom agar/RPMI to prevent the adhesion of cells to culture plates. Medium was changed 3 times a week, and visible colonies were counted after 4 weeks.

Published OnlineFirst October 19, 2016; DOI: 10.1158/1078-0432.CCR-16-1317

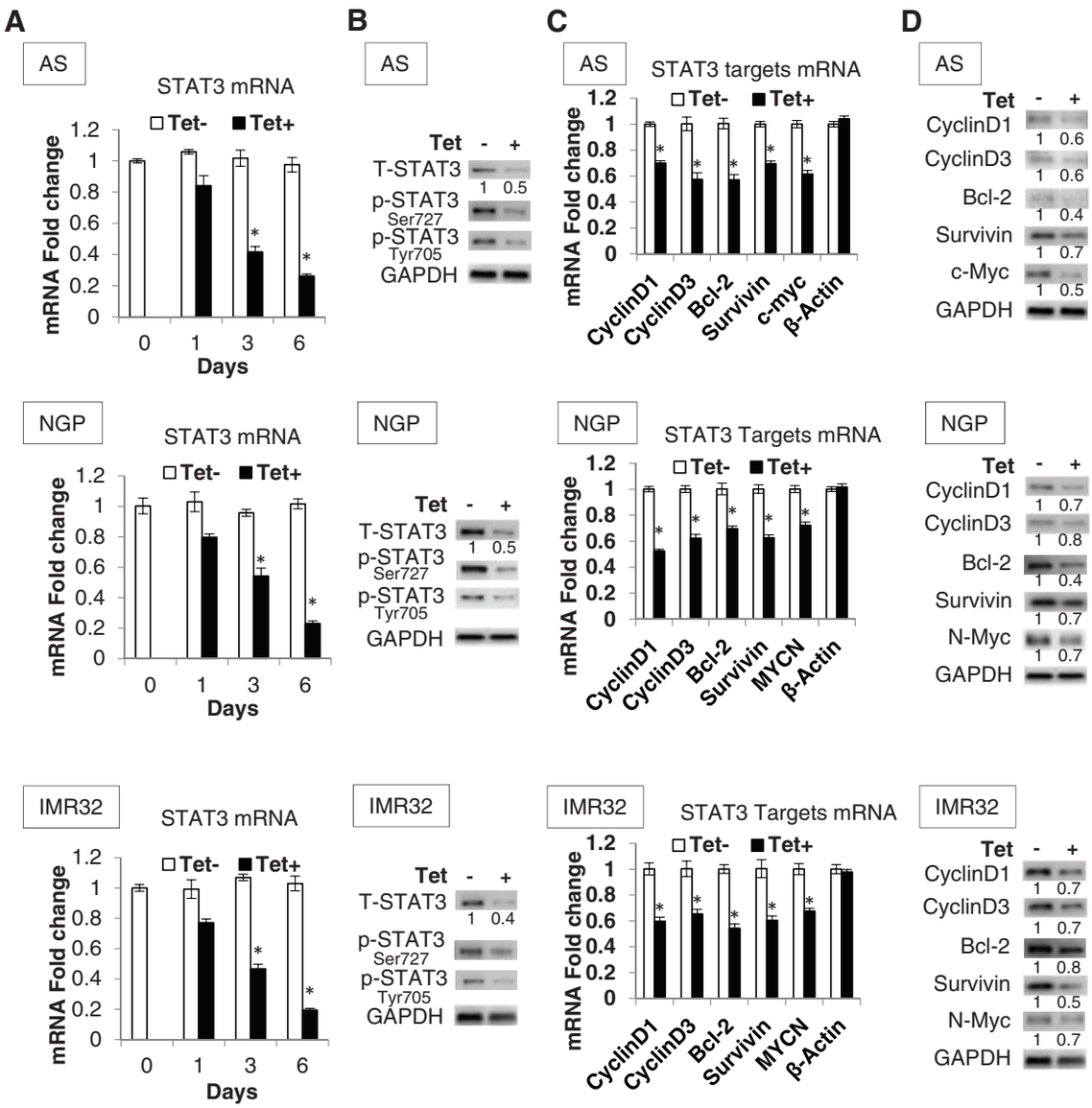

Figure 1.

Downregulation of STAT3 and STAT3 targets after TET induction of shSTAT3 in neuroblastoma cell lines *in vitro*. **A,** STAT3 mRNA expression in neuroblastoma cells expressing Tet-inducible STAT3 shRNA was validated by qPCR. Cells were treated with Tet (1 μg/mL) or solvent control 1, 3, and 6 days before harvesting. The data are presented as the mean of 3 replicate tests ± SE. *, $P < 0.05$ was indicated for Tet-treated cells versus control cells (*t* test). **B,** STAT3 protein expression in cells treated with Tet (1 μg/mL) or solvent control for 6 days was validated by immunoblotting. Ratios of T-STAT3/GAPDH shown under the representative blots were normalized to that of untreated control (normalized as "1") in each cell line. **C,** STAT3 target mRNA expression cells expressing Tet-inducible STAT3 shRNA treated with Tet (1 μg/mL) or solvent control for 6 days was validated by qPCR. The data are presented as the mean of 3 replicate tests ± SE. *, $P < 0.05$ was indicated for Tet-treated cells versus control cells (*t* test). **D,** STAT3 target protein expression in cells treated with Tet (1 μg/mL) or solvent control for 6 days was validated by Western blotting. Ratios of the detected target/GAPDH shown under the representative blots were normalized to that of untreated control (normalized as "1") in each cell line.

Real-time PCR and protein analyses

Total RNA was extracted using RNeasy Mini Kit (Qiagen) and reverse-transcribed to cDNA with SuperScript III First-Strand Synthesis SuperMix (Invitrogen). The levels of mRNA expression of STAT3 target gene cyclin D1, cyclin D3, Bcl-2, survivin, c-myc, and N-myc in neuroblastoma cells treated with AZD9150 or ntASO, and stable clones treated with or without Tet (1 μg/mL) were evaluated by quantitative real-time PCR (qPCR) using an ABI Prism 7000 (Applied Biosystems) with SYBR Green SuperMix according to the manufacturer's protocol. HPRT-1 was used for input normalization, and β-actin was used for negative control. Validated primers used for detection were obtained from RealTimePrimers.com. All qPCR was performed in triplicate.

Proteins (15 μg) were separated by SDS-PAGE gels and then transferred to nitrocellulose membranes. Membranes were

Published OnlineFirst October 19, 2016; DOI: 10.1158/1078-0432.CCR-16-1317

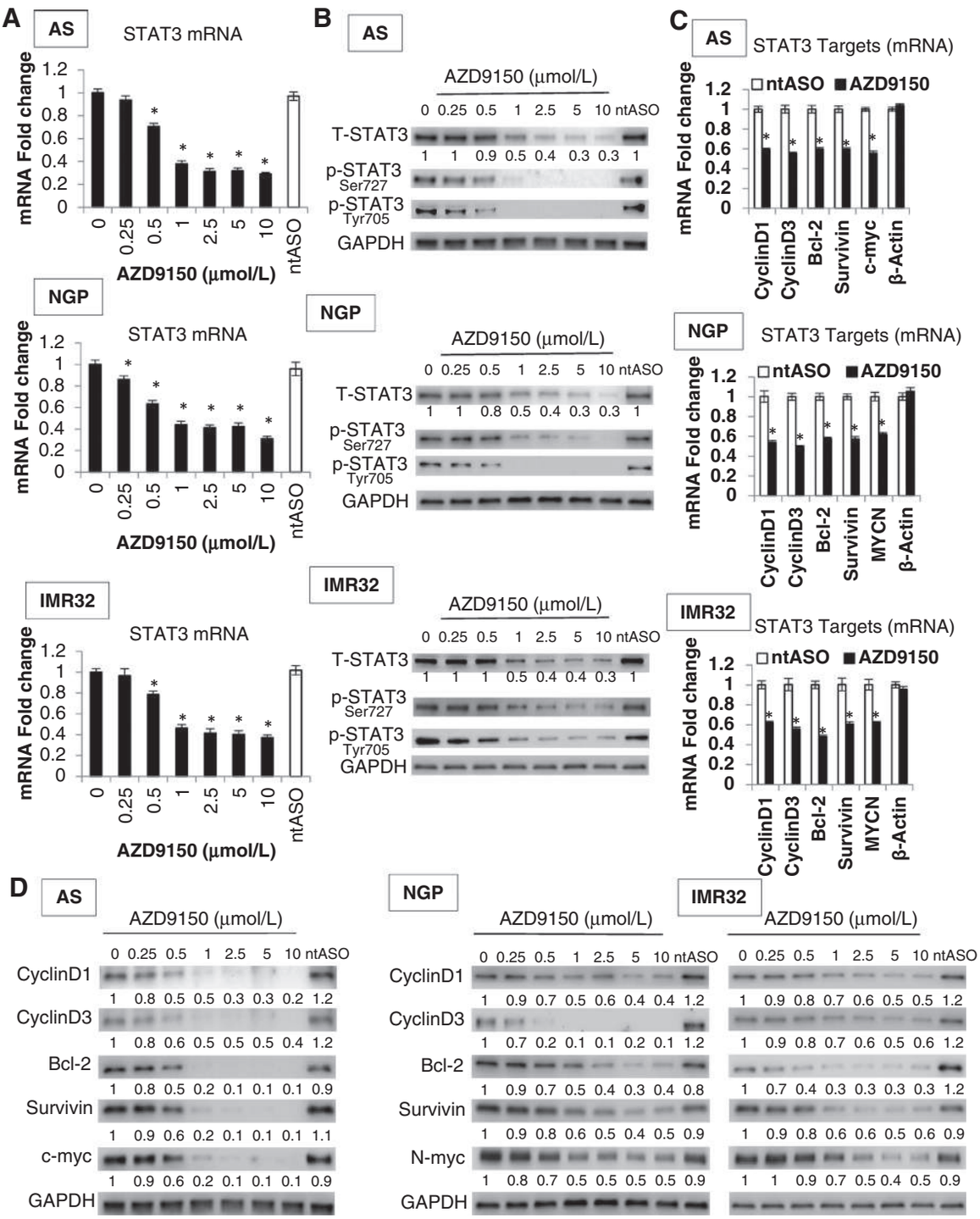

Figure 2.

Downregulation of STAT3 and STAT3 targets by AZD9150 treatment *in vitro*. **A,** STAT3 mRNA expression in neuroblastoma cell lines treated with AZD9150 (0.25, 0.5, 1, 2.5, 5, 10 μmol/L) or ntASO (10 μmol/L) for 6 days was validated by qPCR. The data are presented as the mean of 3 replicate tests ± SE. *, $P < 0.05$ was indicated for AZD9150-treated cells versus control cells (*t* test). **B,** STAT3 protein expression in neuroblastoma cell lines treated with AZD9150 (0.25, 0.5, 1, 2.5, 5, 10 μmol/L) or ntASO (10 μmol/L) for 6 days was validated by Western blotting. Ratios of T-STAT3/GAPDH shown under the representative blots were normalized to that of untreated control (normalized as "1") in each cell line. **C,** STAT3 target mRNA expression in neuroblastoma cell lines treated with AZD9150 (1 μmol/L) or ntASO (1 μmol/L) for 6 days was validated by qPCR. The data are presented as the mean of 3 replicate tests ± SE. *, $P < 0.05$ was indicated for AZD9150-treated cells versus ntASO-treated cells (*t* test). **D,** STAT3 target protein expression in neuroblastoma cell lines treated with AZD9150 (1 μmol/L) or ntASO (1 μmol/L) for 6 days was validated by Western blotting. Ratios of the detected target/GAPDH shown under the representative blots were normalized to that of untreated control (normalized as "1") in each cell line.

Published OnlineFirst October 19, 2016; DOI: 10.1158/1078-0432.CCR-16-1317

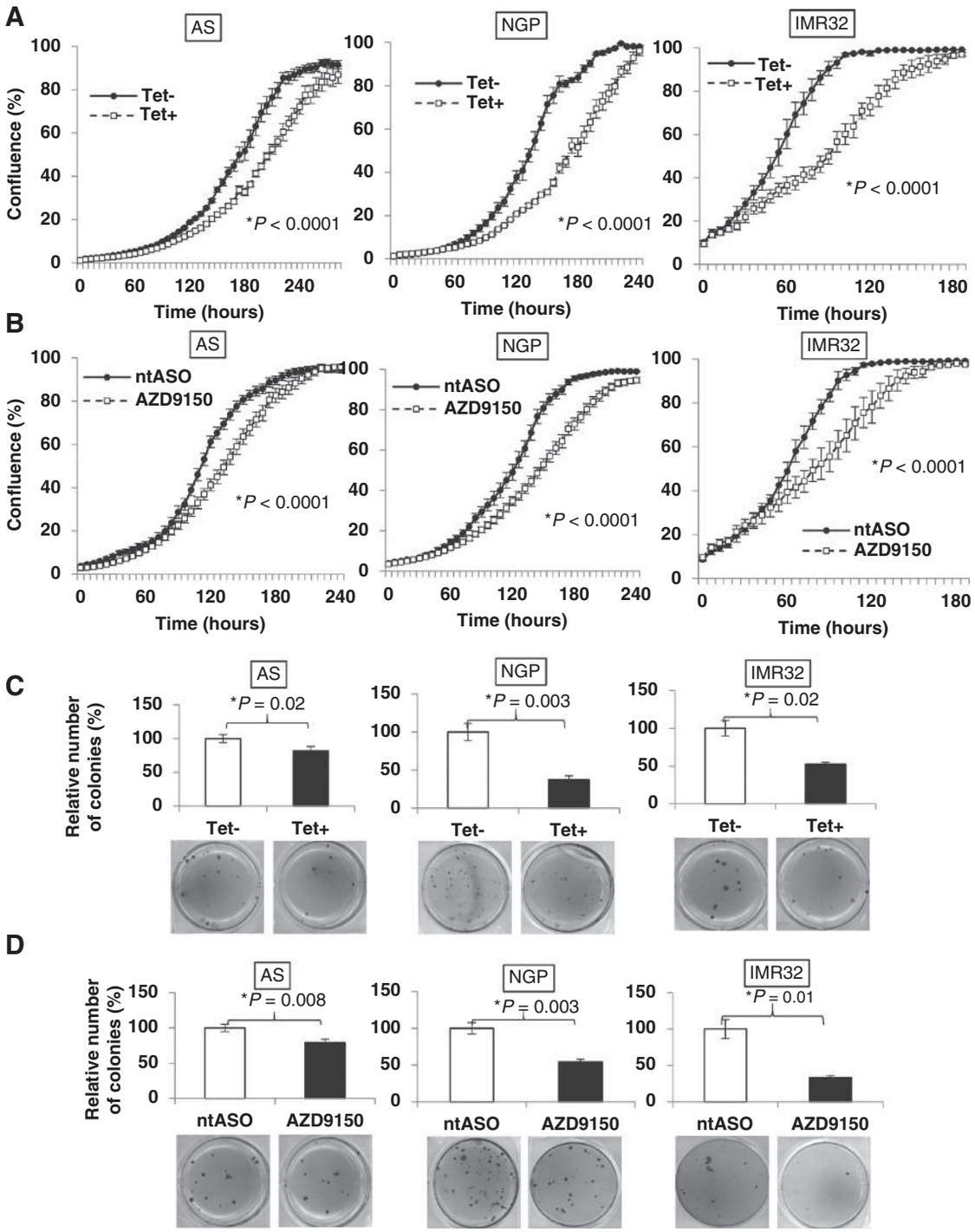

Figure 3.

Genetic or pharmacologic inhibition of STAT3 inhibits neuroblastoma cell growth on plastic and colony formation in soft agar. **A,** Growth of neuroblastoma cells expressing Tet-inducible STAT3 shRNA with Tet (1 μg/mL) or solvent control was measured using IncuCyte (Essen BioSciences) every 6 hours. *P* value between solvent control and Tet-treated group was determined by a 2-way ANOVA. **B,** Growth of neuroblastoma cells treated with AZD9150 (1 μmol/L) or ntASO (1 μmol/L) was measured using IncuCyte (Essen BioSciences) every 6 hours. *P* value between solvent control and Tet-treated group was determined by a 2-way ANOVA. **C,** Colony formation of neuroblastoma cells expressing Tet-inducible STAT3 shRNA in soft agar. Top, Numbers of colonies were counted 4 weeks later of Tet or solvent control treatment. The number of colonies of control cells was taken as 100%. The data are presented as the mean of 3 replicate tests ± SE. *, $P < 0.05$ was indicated for Tet-treated cells versus control cells (*t* test). Bottom, Colonies in the soft agar of a representative image. **D,** Colony formation of neuroblastoma cells treated with AZD9150 or ntASO in soft agar. Top, Numbers of colonies were counted 4 weeks later of AZD9150 (1 μmol/L) or ntASO (1 μmol/L) treatment. The number of colonies of cells with ntASO treatment was taken as 100%. The data are presented as the mean of 3 replicate tests ± SE. *, $P < 0.05$ was indicated for Tet-treated cells versus control cells (*t* test). Bottom, Colonies in the soft agar of a representative image.

Published OnlineFirst October 19, 2016; DOI: 10.1158/1078-0432.CCR-16-1317

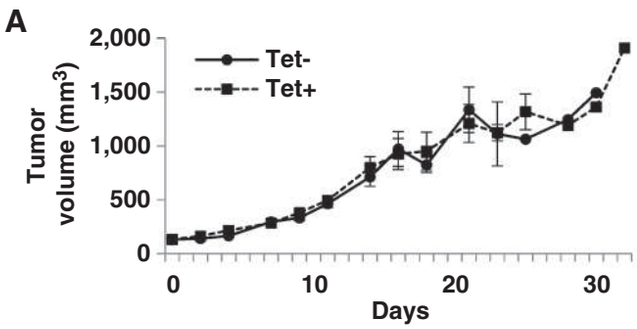

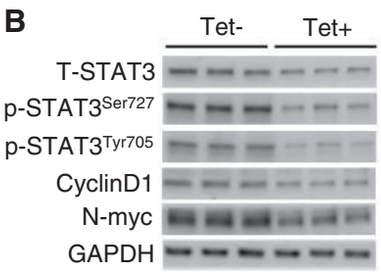

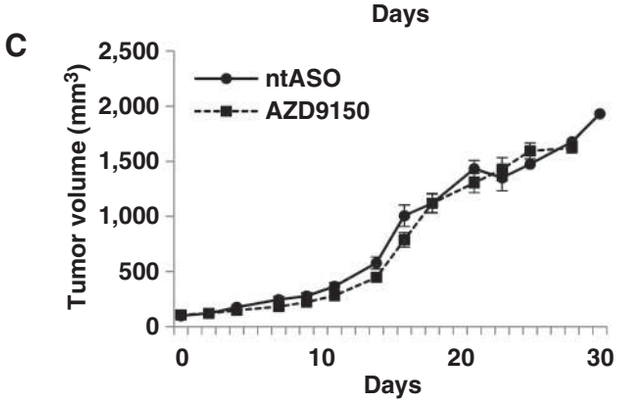

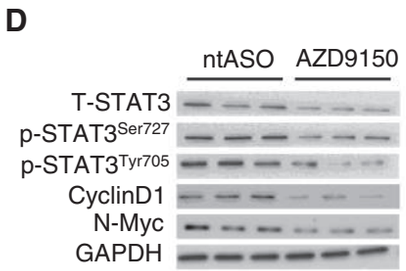

E

The number of mice bearing tumor

	Number of cells injected				
	2×10^6	2×10^5	2×10^4	2×10^3	2×10^2
ntASO	5/5	5/5	4/5	3/5	2/5
AZD9150	5/5	3/5	1/5	0/5	0/5

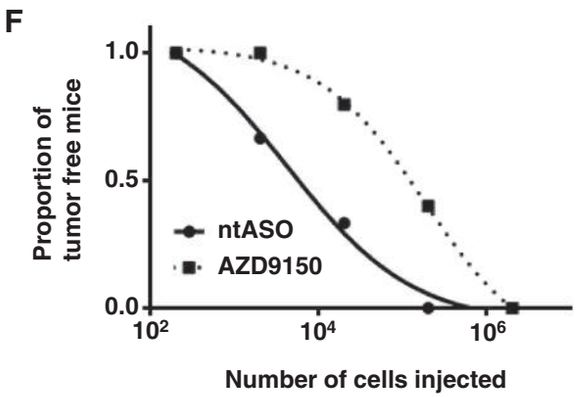

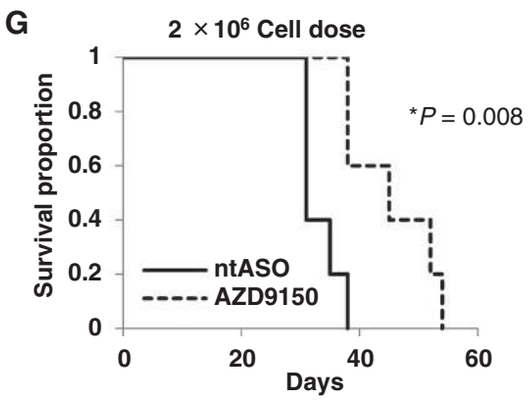

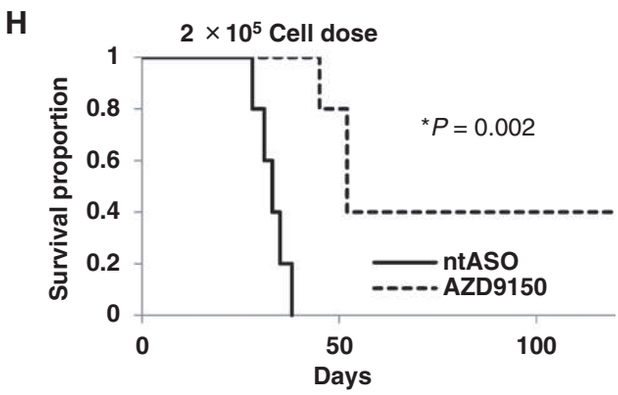

Figure 4.

AZD9150-treated tumors have decreased ability to initiate secondary tumors. **A,** Subcutaneous xenografts of neuroblastoma were established by injection of 2×10^6 cells of NGP-expressing Tet-inducible STAT3 shRNA into the right flank of 5- to 6-week-old female nude mice. Mice were given water supplemented with food containing doxycycline (Tet+) or regular food (Tet−) 1 week before tumor implantation and continued this way throughout the experiment. The graph represents a comparison of mean tumor volumes between normal food (Tet−) or doxycycline food treatment groups (Tet+). The days were counted when the size of the tumors reached 100 to 200 mm^3. Data represent mean ± SE of $n = 7$. **B,** Tumors from Tet− mice cohort or Tet+ mice cohort were excised and proteins were extracted as detailed in Materials and Methods. Total proteins (15 μg) were analyzed by immunoblotting. (*Continued on the following page.*)

Published OnlineFirst October 19, 2016; DOI: 10.1158/1078-0432.CCR-16-1317

blocked with 5% non-fat milk in TBST (0.01% Tween) for 1 hour, incubated with primary antibodies overnight at 4°C, followed by 1-hour incubation with HRP-conjugated secondary antibodies, and then developed with Western Lighting-ECL (Perkin Elmer). Densitometric analysis of appropriately exposed autoradiographs was performed using NIH Image 1.63 software. Relative protein levels (STAT3/GAPDH, cyclin D1/GAPDH, cyclin D3/GAPDH, Bcl-2/GAPDH, survivin/GAPDH, c-myc/GAPDH, and N-myc/GAPDH) were calculated from quantified data. Ratios shown under the representative blots were normalized to that of untreated control (normalized as "1") in each cell line. The concentration of half-maximal inhibition of STAT3 (IC_{50}) was determined by using Prism 6.0 software (GraphPad Software Inc.).

In vivo animal model

For neuroblastoma xenograft model, 5- to 6-week-old female athymic nude mice (Taconic) were injected subcutaneously with 2×10^6 cells (NGP-expressing Tet-inducible STAT3shRNA and NGP). For NGP-expressing Tet-inducible STAT3 shRNA xenografts, mice were given food containing doxycycline or regular food. Treatment began when the subcutaneous tumors reached 100 to 200 mm^3, which was approximately 11 days after implantation. AZD9150 or ntASO (100 mg/kg, 5×/wk) were administered subcutaneously and cisplatin (2 mg/kg, 2×/wk) was given by intraperitoneal injection. Mice tolerated all treatment conditions. Tumor size was measured 3 times a week using calipers, and tumor volume (mm^3) was calculated as $(L \times W^2)/4$, where L = length (millimeter) and W = width (millimeter). Subcutaneous implantation is a heterotypic tumor site for neuroblastoma, but it was chosen to facilitate drug delivery and tumor measurements to assess the effects of pharmacologic or genetic inhibition of STAT3 on tumor growth.

To determine the effect of STAT3 inhibition on survival of tumor-bearing mice, we counted the days from the initiation of treatment to the time the tumors reached a diameter of 2 cm (end point as required by NIH Animal Care and Use Committee). Tumor tissue isolated at the time of euthanasia was stored at −80°C for protein or RNA analyses. All xenograft studies (protocol PB-023) were approved by the Animal Care and Use Committee of the NCI in accordance with the institutional guidelines.

Secondary tumor mouse models were established to determine the effect of AZD9150 on tumor initiation *in vivo*. Female athymic nude mice (5- to 6-week-old; Taconic) were injected subcutaneously with 2×10^6 NGP cells. Subcutaneous tumors from mice treated with AZD9150 (100 mg/kg) or ntASO (100 mg/kg) for 3 weeks were harvested when they reached 2 cm in diameter and cut into pieces under aseptic conditions. After washing with PBS, the tumors were rinsed with RPMI and minced. Cells were filtered through a 40-μm nylon mesh, washed with PBS and viable cells enumerated. Suspensions of cells were mixed with an equal volume of Matrigel solution (Trevigen) and injected subcutaneously in 6-week-old female athymic nude mice (final cell doses 2×10^6, 2×10^5, 2×10^4, 2×10^3, and 2×10^2). Mice were monitored 3 times a week for evidence of tumor formation.

Evaluation and statistical analysis

Analyses were performed using GraphPad Prism 6.0 software. Statistical significance was established at $P < 0.05$.

Results

Tet-inducible STAT3 shRNA decreases endogenous STAT3 and STAT3 targets

Varying levels of total STAT3 and activated, phosphorylated STAT3 (Ser727 and Tyr705) were detected in the 14 neuroblastoma cell lines evaluated (Supplementary Fig. S1A). Three cell lines, SK-N-AS (single copy-MYCN), NGP (MYCN-amplified), and IMR32 (MYCN-amplified), were selected to study the effects of specific STAT3 inhibition in neuroblastoma. The cell lines grown under our culture conditions contain readily detected levels of phosphorylated STAT3 (P-STAT3) that is found in cytosolic and nuclear compartments (Supplementary Fig. S1B). We first analyzed STAT3 mRNA levels in 3 neuroblastoma cell stable clones (AS, NGP, and IMR32) expressing a Tet-inducible STAT3 shRNA (Tet-shSTAT3). STAT3 mRNA levels were significantly decreased within 3 to 6 days of Tet treatment in each neuroblastoma cell line evaluated (Fig. 1A). In the presence of Tet, there was a 50% to 60% decrease in both total STAT3 and phosphorylated STAT3 (Ser727 and Tyr705) protein levels (Fig. 1B). To determine whether inhibition of STAT3 affected the transcription of STAT3 target gene expression, we analyzed the expression of selected STAT3 target genes (cyclin D1, cyclin D3, Bcl-2, survivin, c-myc, and MYCN) by qPCR and immunoblots. After 6 days of Tet treatment, there was a decrease in the mRNA (Fig. 1C) and protein (Fig. 1D) levels of STAT3 target genes. These data indicate that STAT3 genetic inhibition suppressed STAT3 phosphorylation and expression of STAT3 downstream targets.

To determine whether there was differential expression of STAT3 in the neuroblastoma cell populations, we analyzed total and phosphorylated STAT3 by immunocytofluorescence. In the absence of Tet, all of AS, NGP, and IMR32 neuroblastoma Tet-STAT3shRNA cells were positive for total and phosphorylated STAT3 (Supplementary Fig. S2A, S2E, and S2I), whereas in the presence of TET, there was uniform inhibition of total and P-STAT3 levels in the neuroblastoma cells (Supplementary Fig. S2B, S2F, and S2J). This indicates that in each of the cell lines, the majority of cells express activated STAT3, which is inhibited uniformly by STAT3 shRNA after Tet treatment.

AZD9150 inhibits endogenous STAT3 and STAT3 targets

AZD9150 is a first-in-class STAT3-targeted ASO that is currently in phase I clinical trials (NCT01839604). SK-N-AS, NGP, and

(*Continued.*) **C,** Subcutaneous xenografts of neuroblastoma were established by injection of 2×10^6 cells of NGP into the right flank of 5- to 6-week-old female nude mice. The ntASO or AZD9150 treatments were initiated when tumors reached 100 to 200 mm^3. Either ntASO (100 mg/kg) or AZD9150 (100 mg/kg) were subcutaneously injected into mice once a day for 5 days a week for 3 weeks. The graph represents a comparison of mean tumor volumes between ntASO (100 mg/kg) and AZD9150 (100 mg/kg) treatment groups (Tet+). Data represent mean ± SE of $n = 10$. **D,** Tumors of ntASO-treated group or AZD9150-treated group were excised and protein was extracted as detailed in Materials and Methods. Total protein (15 μg) was analyzed by immunoblotting. **E,** Female athymic nude mice were injected subcutaneously with 2×10^6 NGP cells. Subcutaneous tumors treated with AZD9150 (100 mg/kg) or ntASO (100 mg/kg) for 3 weeks were harvested and injected subcutaneously to new athymic nude mice (final cell doses 2×10^6, 2×10^5, 2×10^4, 2×10^3, and 2×10^2). The numbers in the table represent the number of animals developing tumors over the number of animals injected with the indicated number of tumor cells. **F,** Limiting dilution analysis of 2 groups. Each symbol represents a proportion of tumor-free mice transplanted with 2×10^2, 2×10^3, 2×10^4, 2×10^5, and 2×10^6 cells. **G** and **H,** Survival curve was plotted by Kaplan–Meier analysis. *P* value was calculated using a 2-sided log-rank test. Time taken for tumor initiation and survival was measured up to 120 days.

Published OnlineFirst October 19, 2016; DOI: 10.1158/1078-0432.CCR-16-1317

IMR32 neuroblastoma cells were treated with various concentrations of AZD9150 (0.25–10 μmol/L) and ntASO, a nontargeted siRNA control (10 μmol/L). AZD9150 treatment inhibited STAT3 mRNA levels in a dose-dependent manner (Fig. 2A). The AZD9150 IC_{50} values of STAT3 mRNA inhibition in AS, NGP, and IMR32 are 0.69, 0.64, 0.76 μmol/L, respectively. AZD9150 also decreased both total and phosphorylated STAT3 protein levels in a dose-dependent manner (Fig. 2B). AZD9150 also inhibited IL6-mediated increases in phosphorylation of STAT3 (Supplementary Fig. S1C). The AZD9150 IC_{50} values of STAT3 protein inhibition in AS, NGP, and IMR32 are 0.99, 0.97, 0.98 μmol/L, respectively. We selected 1 μmol/L of AZD9150 to analyze the expression of selected STAT3 target genes (cyclin D1, cyclin D3, Bcl-2, survivin, c-myc, and MYCN) by qPCR. AZD9150 treatment significantly decreased mRNA (Fig. 2C) and protein (Fig. 2D) levels of STAT3 target genes compared with ntASO treatment. Next, we analyzed total and phosphorylated STAT3 by immunocytofluorescence. In the presence of ntASO (1 μmol/L), all AS, NGP, and IMR32 cells were positive for total and phosphorylated STAT3 (Supplementary Fig. S2C, S2G, and S2K), but in the presence of AZD9150 (1 μmol/L), there was uniform inhibition of total and P-STAT3 levels in the neuroblastoma cells (Supplementary Fig. S2D, S2H, and S2L). These data are consistent with findings using the shSTAT3 neuroblastoma cell lines (Fig. 1, Supplementary Fig. S2). Both genetic (shSTAT3) and pharmacologic (AZD9150) treatments caused decreases in STAT3 levels causing a reduction in phosphorylation of STAT3 and inhibition of STAT3 target gene expression.

The effects of genetic and AZD9150 inhibition of STAT3 on neuroblastoma cell growth and tumorigenicity

To assess the effects of STAT3 genetic inhibition on growth of neuroblastoma cells, we monitored confluence of stable clones (AS, NGP, IMR32) expressing Tet-inducible STAT3 shRNA using the IncuCyte system. Tet-inducible STAT3 shRNA significantly decreased cell growth of these neuroblastoma cells (up to 37% decrease, $P < 0.0001$ in AS, up to 52% decrease, $P < 0.0001$ in NGP, up to 48% decrease, $P < 0.001$ in IMR32; Fig. 3A). We next monitored growth of neuroblastoma cells treated with AZD9150 (1 μmol/L) or ntASO (1 μmol/L). AZD9150 treatment resulted in a significant decrease in the growth of these neuroblastoma cells (up to 38% decrease, $P < 0.0001$ in AS, up to 37% decrease, $P < 0.0001$ in NGP, up to 34% decrease, $P < 0.0001$ in IMR32; Fig. 3B). We next assessed the effect of STAT3 inhibition on anchorage-independent neuroblastoma cell growth using a soft agar assay. The number of colonies in the presence of Tet was significantly reduced in AS (19% decrease, $P = 0.02$), NGP (62% decrease, $P = 0.003$), and IMR32 (47% decrease, $P = 0.02$) expressing Tet-inducible STAT3 shRNA neuroblastoma cell lines (Fig. 3C). AZD9150 significantly reduced the number of colonies compared with ntASO treatment groups in AS (20% decrease, $P = 0.008$), NGP (43% decrease, $P = 0.003$), and IMR32 (67% decrease, $P = 0.01$; Fig. 3D). These data indicate that STAT3 inhibition slows growth *in vitro* and inhibits the ability of neuroblastoma cells to form colonies in soft agar.

Cell migration is an important process in the tumorigenic and metastatic capability of neuroblastoma cells. The effect of STAT3 inhibition on cell migration was evaluated using a scratch wound assay. We found a small but significant inhibition of cell migration when levels of STAT3 were decreased in our shSTAT3 models (Supplementary Fig. S3A) or when treated with AZD9150 (Supplementary Fig. S3B). Thus, a decrease in STAT3 expression inhibits neuroblastoma cell colony-forming ability in soft agar as well as neuroblastoma cell migration.

Decreased tumor-initiating capability of neuroblastoma cells from AZD9150-treated tumors

We next tested the effect of STAT3 genetic inhibition on tumor growth *in vivo*. NGP-expressing Tet-inducible STAT3 shRNA cells were injected into nude mice that were treated with or without Tet. STAT3 genetic inhibition alone did not affect tumor growth *in vivo* (Fig. 4A). To evaluate the effect of shRNA targeting STAT3 *in vivo*, we collected tumor samples from mice treated with or without Tet. We verified that the protein levels of total and phosphorylated STAT3 and STAT3 targets cyclin D1 and N-myc in tumors from mice treated with Tet were decreased compared with tumors from non–Tet-treated mice (Fig. 4B). Next, we evaluated whether AZD9150 (100 mg/kg) would affect the growth of established tumors. NGP neuroblastoma cells were implanted into mice and when tumors reached 100 to 200 mm were treated with AZD9150 or ntASO (100 mg/kg) 5 days per week for 3 weeks. As shown in Fig. 4C, AZD9150 treatment did not affect the growth of established tumors. The protein levels of total and phosphorylated STAT3 and STAT3 targets were decreased with AZD9150 treatment and these resulted in decreases in STAT3 targets MYCN and cyclin D1 protein expression (Fig. 4D).

Although inhibition of STAT3 did not alter growth of established tumors, AZD9150 treatment did decrease colony formation in soft agar *in vitro* (Fig. 3D), suggesting that inhibition of STAT3 may alter the ability of neuroblastoma cells to initiate tumor growth. To assess tumor initiation, tumors were removed after the 3-week ntASO or AZD9150 (100 mg/mL) treatment and secondary tumor formation assessed by implanting different cell doses (2×10^6, 2×10^5, 2×10^4, 2×10^3, and 2×10^2 cells) into mice. The number of tumor-bearing mice and the proportion of tumor-free mice are shown in Fig. 4E and F. Limiting dilution analysis indicates a significant difference in the precursor frequency of tumor-initiating cells: 1 of 5,178 in the ntASO-treated neuroblastoma cells and 1 of 187,030 in AZD9150-treated neuroblastoma cells ($P = 1.9e{-}08$ by χ^2 analysis). STAT3 inhibition caused an almost 30-fold decrease in the precursor frequency of neuroblastoma tumor-initiating cells *in vivo*. The survival of mice injected at doses of 2×10^6 and 2×10^5 cells was significantly longer in the AZD9150-treated group than in the ntASO-treated group (Fig. 4G) At the 2×10^5 cell dose, all the mice receiving ntASO-treated tumor cells had to be euthanized at 58 days, whereas 40% of the mice receiving AZD9150-treated tumor cells were tumor-free at 58 days (Fig. 4H) and remained tumor-free to 120 days when the experiment was terminated (data not shown). These data are consistent with inhibition of STAT3 affecting the tumor-initiating capability of NGP neuroblastoma cells.

Tet-inducible STAT3 shRNA or AZD9150 increased chemosensitivity *in vitro*

It has been shown that STAT3 inhibition sensitizes cancer cells to chemotherapeutic agents. We therefore evaluated whether STAT3 genetic inhibition or AZD9150 would sensitize neuroblastoma cell lines to cisplatin, which is commonly used in the therapies for high-risk neuroblastoma and carries with it significant toxicities. The viability of NGP-expressing Tet-inducible STAT3 shRNA treated with or without Tet and then treated with cisplatin was evaluated by MTS assay. The

Published OnlineFirst October 19, 2016; DOI: 10.1158/1078-0432.CCR-16-1317

combination of Tet and cisplatin significantly inhibited cell viability (Fig. 5A), as did the combination of AZD9150 and cisplatin (Fig. 5B). Similar results were seen in AS and IMR32 cells (Supplementary Fig. S4A and S4B). Next, we evaluated cell viability at various cisplatin concentrations (0–10 μg/mL). Tet-inducible STAT3 shRNA-mediated decreases in STAT3 resulted in

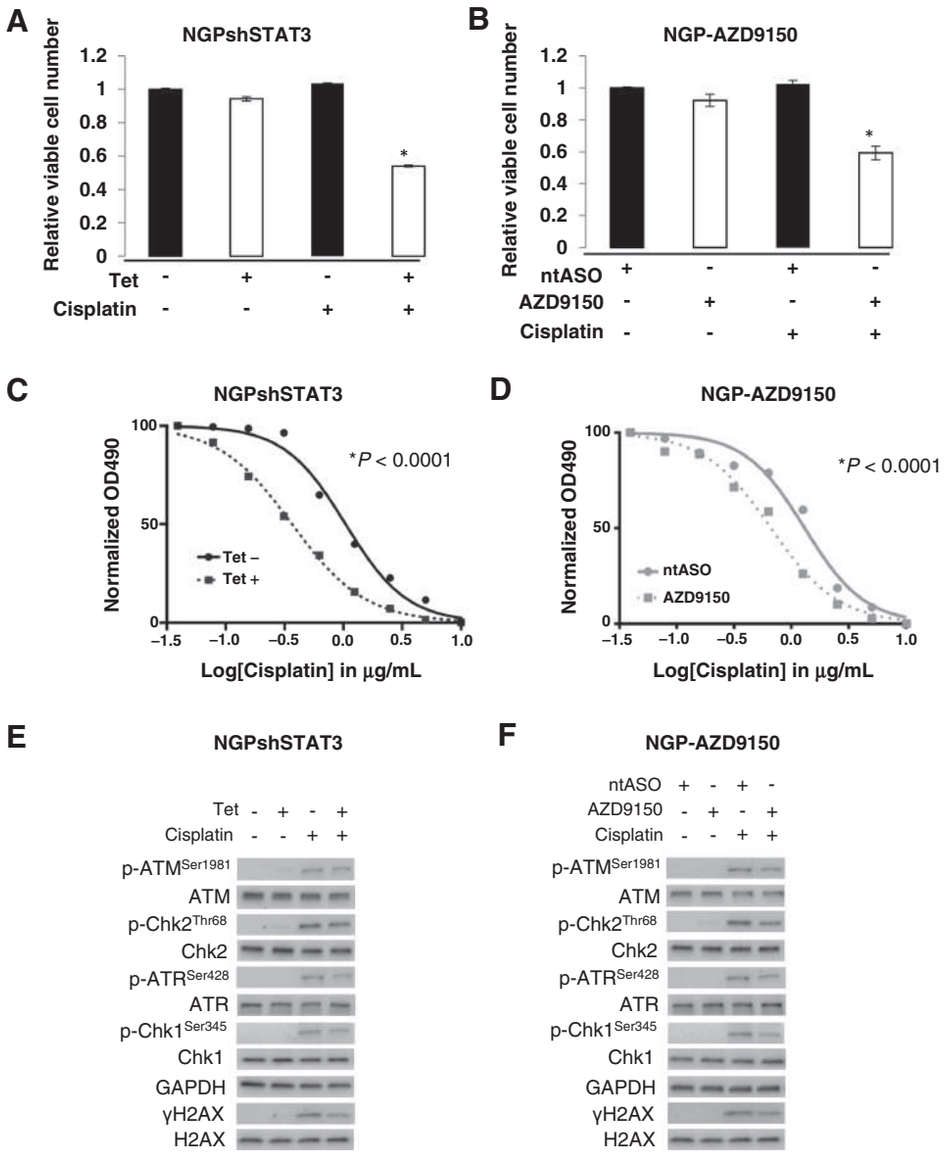

Figure 5.

Genetic or pharmacologic inhibition of STAT3 increased chemosensitivity *in vitro*. **A,** Relative number of NGP Tet-shSTAT3 cells cultured in the presence of Tet (1 μg/mL) or solvent for 3 days followed by a treatment with control solvent or cisplatin (0.3 μg/mL) was evaluated using an MTS assay. Relative cell number was normalized to untreated cells. The data are presented as the mean of 3 replicate tests ± SD. Statistical significance (*, $P < 0.05$) is indicated for the combination of Tet and cisplatin-treated cells versus control cells (*t* test). **B,** NGP cells were treated with AZD9150 (1 μmol/L) or ntASO (1 μmol/L) for 3 days followed by treatment with cisplatin (0.3 μg/mL) or control solvent for an additional 3 days. Relative cell numbers were assessed using an MTS assay. Relative cell number was normalized to ntASO-treated and solvent-treated cells. The data are presented as the mean of 3 replicate tests ± SD. Statistical significance (*, $P < 0.05$) is indicated for the combination of AZD9150- and cisplatin-treated cells versus ntASO, solvent-treated cells (*t* test). **C,** NGP-expressing Tet-inducible STAT3 shRNA cells were treated with Tet (1 μg/mL) or solvent control and cultured for 3 days followed by an additional 3-day incubation with various concentrations of cisplatin. Relative cell numbers were assessed by MTS assay and values normalized to the value of untreated cells. *P* value was determined using a 2-way ANOVA test. **D,** NGP cells were treated with AZD9150 (1 μmol/L) or ntASO (1 μmol/L) for 3 days followed by a 3-day cultured with varying concentrations of cisplatin. Relative cell numbers were evaluated using an MTS assay and values normalized to the respective values for AZD9150 or ntASO in the absence of cisplatin. *P* value was determined using a 2-way ANOVA test. **E,** NGP-expressing Tet-inducible STAT3 shRNA was treated with Tet or control for 3 days followed by cisplatin (0.3 μg/mL) in combination for another 3 days, and then total protein was extracted. Total protein (15 μg) was analyzed by immunoblotting. **F,** NGP cells were treated with AZD9150 (1 μmol/L) or ntASO (1 μmol/L) for 3 days followed by cisplatin (0.3 μg/mL) in combination for another 3 days, and then total protein was extracted. Total protein (15 μg) was analyzed by immunoblotting.

Published OnlineFirst October 19, 2016; DOI: 10.1158/1078-0432.CCR-16-1317

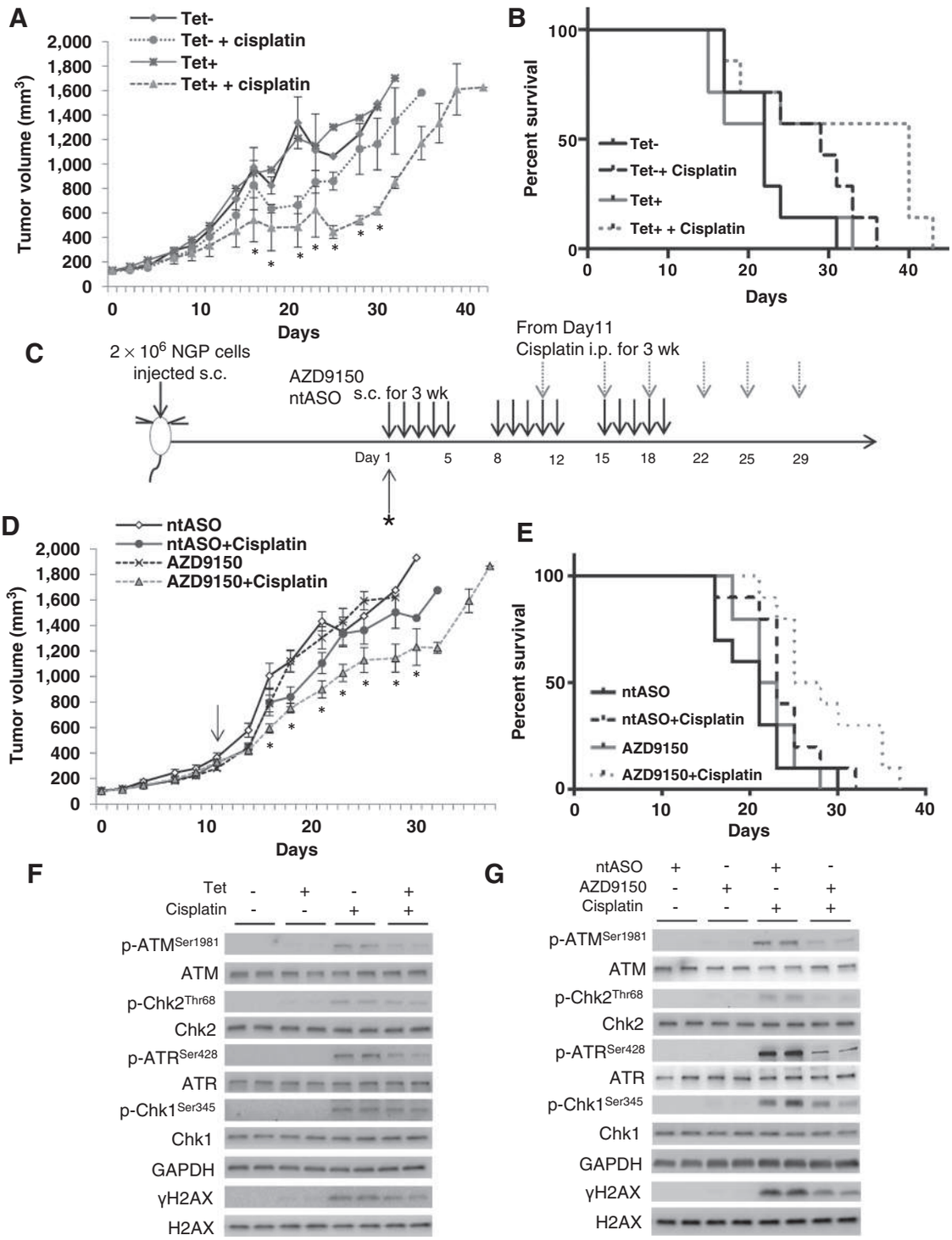

Figure 6.

Genetic or pharmacologic inhibition of STAT3 increased chemosensitivity *in vivo*. **A,** Subcutaneous xenografts of neuroblastoma were established by injection of 2×10^6 NGP-expressing Tet-inducible STAT3 shRNA cells into the right flank of 5- to 6-week-old female nude mice. Mice were given water supplemented with food containing doxycycline (Tet+) or regular food (Tet−) 1 week before tumor implantation which was continued throughout the experiment. Cisplatin treatment (2 mg/kg) was initiated when tumors reached 100 to 200 mm^3. Cisplatin (2 mg/kg) was injected twice a week intraperitoneally. The tumor size in treated groups was compared with that of Tet− group. Data represent mean ± SE of $n = 7$ mice per cohort. *P* value was calculated using the Student *t* test. *, $P < 0.05$ was indicated for the combination of Tet+ and cisplatin-treated mouse versus Tet− mouse. (*Continued on the following page.*)

Published OnlineFirst October 19, 2016; DOI: 10.1158/1078-0432.CCR-16-1317

a 2- to 3-fold decrease in the cisplatin IC_{50} in the neuroblastoma cell lines (AS (0.87–0.39 μg/mL, $P < 0.0001$), NGP (1.04–0.37 μg/mL, $P < 0.0001$), IMR32 (1.65–0.76 μg/mL, $P < 0.0001$; Fig. 5C, Supplementary Fig. S4C). Inhibition of STAT3 using 1 μmol/L AZD9150 resulted in a 2-fold decrease in the cisplatin IC_{50} compared with ntASO-treated cells (NGP, 1.30–0.65 μg/mL $P < 0.0001$ and IMR32, 1.15–0.49 μg/mL, $P < 0.0001$), with a smaller effect on cisplatin sensitivity of AS cells (from 0.22 to 0.17 μg/mL, $P = 0.0063$; Fig. 5D, Supplementary Fig. S4D). These results indicate that STAT3 genetic or pharmacologic AZD9150-mediated inhibition of STAT3 enhances chemosensitivity to cisplatin in neuroblastoma cells.

The DNA damage response pathway is activated after cisplatin induced DNA strand breaks. To elucidate mechanisms by which STAT3 inhibition might enhance the sensitivity of neuroblastoma cells to cisplatin, we evaluated the DNA damage response pathway by Western blot analysis. In response to DNA damage, ATM and ATR are activated leading to activation of H2AX as well as their respective downstream targets Chk2 and Chk1 (33, 34). Activation of both the ATM and ATR DNA damage response pathways are detected after cisplatin treatment as indicated by the increases in phosphorylation of their respective downstream targets. However, genetic or pharmacologic inhibition of STAT3 attenuated the activation of the DNA damage response pathway by cisplatin (Fig. 5E and F).

Inhibition of STAT3 sensitizes neuroblastoma tumor xenografts to cisplatin treatment

We further tested the efficacy of the combination of STAT3 genetic inhibition and cisplatin *in vivo*. NGP-expressing Tet-inducible STAT3 shRNA cells were injected into nude mice that were treated with or without Tet. Cisplatin (2 mg/kg) treatment was initiated when the subcutaneous tumors reached 100 to 200 mm^3. While this dose of cisplatin did not cause a statistically significant alteration in the tumor growth as a single agent compared with Tet^- group, the combination of STAT3 genetic inhibition and cisplatin caused an up to 64% decrease in tumor growth (Fig. 6A). In addition, the combination of STAT3 genetic inhibition and cisplatin significantly prolonged the survival of tumor-bearing mice (*, $P = 0.04$; Tet^- + vs. Tet^++ cisplatin; Fig. 6B), whereas STAT3 genetic inhibition alone ($P = 0.9$; Tet− vs. Tet+) did not cause a statistically significant alteration in the survival of mice.

Next, we evaluated whether AZD9150 (100 mg/kg) would alter the sensitivity of neuroblastoma tumors to cisplatin. The treatment schedule is depicted in Fig. 6C. NGP cells were subcutaneously injected into nude mice, and AZD9150 or ntASO (100 mg/kg) treatment was initiated when the subcutaneous tumors reached 100 to 200 mm^3. At day 11, cisplatin (2 mg/kg) treatment was initiated and given twice a week. While there was no significant difference in tumor growth between ntASO or the combination of ntASO and cisplatin-treated groups (Fig. 6D), the combination of AZD9150 and cisplatin resulted in a significant decrease (up to 38% decrease) in tumor growth compared with ntASO group. Kaplan–Meier survival curves indicated that the combination of AZD9150 and cisplatin significantly prolonged the survival of mice (*, $P = 0.003$; Fig. 6E). AZD9150 ($P = 0.5$) or cisplatin ($P = 0.08$) used as single agents did not cause statistically significant alterations in murine survival.

To assess the expression of DNA damage response pathway, we examined the murine xenograft tumors (at day 11 of treatment) by Western blot analysis. ATM, Chk2, ATR, Chk1, and γH2AX were phosphorylated by cisplatin, and the levels were reduced in the combination of STAT3 inhibition (Tet-inducible shRNA or AZD9150) and cisplatin (Fig. 6F and G). These results are consistent with *in vitro* results (Fig. 5E and F) and taken together indicate that STAT3-specific inhibition enhances chemosensitivity of neuroblastoma cells to cisplatin *in vivo*.

Discussion

Constitutive activation of STAT3 contributes to tumorigenesis, proliferation, survival, and invasion of various human cancers (8–17); thus, STAT3 is an attractive target in cancer therapy. However, transcription factors have proved to be difficult targets to drug. AZD9150 is a 2.5 generation ASO molecule targeting the 3′-untranslated region of the STAT3 gene, and treatment of human cells results in decreased production of STAT3 protein (28). In this study, we evaluated the efficacy of inhibition of STAT3 using inducible shSTAT3-expressing neuroblastoma cell lines or AZD9150-treated neuroblastoma cell lines. Both strategies decreased endogenous total and phosphorylated STAT3 resulting in diminished expression of STAT3 targets at both the mRNA and the protein levels in neuroblastoma. Our finding that inhibition of STAT3 decreased colony formation *in vitro* and the ability of AZD9150-treated xenograft tumor cells to initiate secondary tumors suggested a dependency of a subset of neuroblastoma tumor–initiating cells on STAT3. Interestingly while inhibition of STAT3 did not affect the growth of established neuroblastoma tumors *in vivo*, when combined with a cytotoxic agent such as cisplatin, the sensitivity of neuroblastoma cells was significantly increased.

Levels of phosphorylated STAT3 in tumor cells are influenced by intrinsic homeostatic regulatory processes as well as paracrine

(*Continued*.) **B,** Survival curves were plotted using a Kaplan–Meier analysis. *P* value was calculated using a 2-sided log-rank test. $P = 0.9$, Tet− versus Tet+; $P = 0.1$, Tet− versus Tet− + cisplatin; *, $P = 0.04$, Tet− versus the combination of Tet+ and cisplatin. **C,** Schematic representation of the experimental plan to assess the efficacy of a combined AZD9150 and cisplatin treatment protocol. Two million NGP cells were injected subcutaneously into female athymic nude mice. When the tumors reached 100 to 200 mm^3, AZD9150 (100 mg/kg) or ntASO (100 mg/kg) treatment was initiated (Day 1). AZD9150 (100 mg/kg) or ntASO (100 mg/kg) was given 5 days a week for 3 weeks. At day 11, cisplatin (2 mg/kg) was given twice a week for 3 weeks. When tumors reached a diameter of 2 cm, mice were euthanized. **D,** Graph represents mean tumor volumes of various treatment cohorts [ntASO (100 mg/kg)-, AZD9150 (100 mg/kg)-, the combination of ntASO (100 mg/kg) and cisplatin (2 mg/kg)-, and the combination of AZD9150 (100 mg/kg) and cisplatin (2 mg/kg)-treated groups]. Arrow shows the day that cisplatin treatment was initiated. Data represent mean ± SE, $n = 10$ mice per cohort. *P* value was calculated using the Student *t* test. *, $P < 0.05$ was indicated for the combination of AZD9150- and cisplatin-treated mouse versus ntASO-treated mouse. **E,** Survival curves were generated using a Kaplan–Meier analysis. *P* value was calculated using a 2-sided log-rank test. $P = 0.5$, ntASO versus AZD9150; $P = 0.08$, ntASO versus the combination of ntASO and cisplatin; *, $P = 0.003$, ntASO versus the combination of AZD9150 and cisplatin. **F,** Tumors from Tet−, Tet+, cisplatin (2 mg/kg), or the combination of Tet+ and cisplatin (2 mg/kg) from 2 mice per cohort were excised and proteins were extracted. Total proteins (15 μg) were analyzed by immunoblotting. **G,** Tumors of ntASO (100 mg/kg), AZD9150 (100 mg/kg), the combination of ntASO (100 mg/kg) and cisplatin (2 mg/kg), or the combination of AZD9150 and cisplatin treatment cohorts were excised and proteins were extracted. Total proteins (15 μg) were analyzed by immunoblotting.

Published OnlineFirst October 19, 2016; DOI: 10.1158/1078-0432.CCR-16-1317

sources of cytokines or growth factors secreted by immune or stromal cells in the tumor microenvironment (30). In neuroblastoma cells, high-level expression of wild-type ALK in cells constitutively expressing putative ALK ligands (31) or mutations in ALK (32) contribute to levels of P-STAT3. Although not systematically studied, growth factors known to be produced by neuroblastoma cells, such as IGF1 (33) and BDNF (ref. 34, our unpublished data), stimulate increases in P-STAT3. These factors as well as growth factors contained in serum may contribute to the levels of P-STAT3 detected in neuroblastoma cells cultured *in vitro*. Paracrine factors found in the tumor microenvironment such as IL6 (22), sphingosine-1-phosphate (35), and G-CSF (24) secreted by immune or stromal cells may contribute to the levels of P-STAT3 in neuroblastoma cells expressing their respective receptors. We found that AZD9150 inhibition of STAT3 results in an almost 50% decrease in STAT3 targets such as cyclin D1, cyclin D3, and c-myc or N-myc, all proteins known to stimulate neuroblastoma cell growth and tumorigenicity. This may account for the 20% to 40% decrease in growth on plastic and 50% decrease in soft agar cloning detected *in vitro*. Despite the fact that cyclin D and N-myc levels decreased, as a single agent, AZD9150 did not significantly alter the growth of established neuroblastoma tumors *in vivo*. That both the genomic and pharmacologic inhibition of STAT3 yielded comparable results indicates that the biologic effects are a direct result of inhibition of STAT3 in the tumor. However, these *in vivo* results contrast with our previous study using the JAK2/STAT3 inhibitor AZD1480 (27) and a recent study using Stattic (25), each of which showed significant antitumor activity *in vivo* as single agents. Unlike these agents, genetic inhibition of STAT3 levels would perturb STAT3 biologic activities mediated by both unphosphorylated STAT3 and phosphorylated STAT3. Recent studies indicate that unphosphorylated STAT3 is capable of binding DNA (reviewed in ref. 30), although the impact of this activity in tumor cells has not been fully explored. In addition, AZD9150 is selective for human STAT3 but not murine STAT3 (28). Because AZD9150 only recognizes sequences in human STAT3 (28), the systemic administration of AZD9150 would not affect STAT3-expressing murine cells in the microenvironment of the human tumor xenograft, raising the possibility that STAT3-expressing cells in the tumor microenvironment are important contributors to xenograft growth. Our future studies will explore the contribution of STAT3-expressing cells in the tumor microenvironment using murine-targeted ASO to STAT3.

Although the inhibition of STAT3 in the tumor did not affect the growth of established neuroblastoma xenografts, we did find that the ability of AZD9150-treated NGP xenograft tumors to initiate secondary tumors was significantly impaired. The ability to form secondary tumors is a property of a tumor-initiating cell or cancer stem–like cell. STAT3 is known to be important for the maintenance of a cancer stem cell–like subpopulation in bladder, colon, hepatocellular, and glial malignancies (18–21), and blockade of STAT3 inhibits tumor initiation in prostate cancer (36). In neuroblastoma, it has been reported that a G-CSF receptor (CD114)–positive subpopulation of neuroblastoma cells has increased tumor-initiating capacity, and inhibition of STAT3 using Stattic affected tumor formation *in vivo* (24, 25). While it is beyond the scope of this study to investigate the phenotypic nature of this tumor-initiating cell, this study provides additional evidence that a subset of neuroblastoma tumor–initiating cells is dependent on STAT3 expression.

Despite the finding that the inhibition of STAT3 in tumors did not affect the growth of established tumors, this study showed that it did increase their sensitivity to cisplatin. This is important because despite the improvements of recent treatment regimens for patients with high-risk neuroblastoma, current multimodality therapeutic protocols remain inadequate for some 50% of patients with high-risk disease and this is, in large part, due to the development of chemoresistance. Moreover, platinum-based cytotoxics are an integral part of induction therapy for these patients but are also associated with severe hearing loss in 67% of patients (37). Resistance to cisplatin has been associated with STAT3 in several solid tumors including breast, colon cancer, non–Hodgkin lymphoma, non-small cell lung cancer, and malignant rhabdoid (38–42). We and others have shown in preclinical models that activated survival signaling pathways contribute to chemoresistance in neuroblastoma cells (29, 43), and our findings that activated STAT3 also alters sensitivity of neuroblastoma cells to cisplatin is consistent with previous results showing that cytokines from bone marrow–derived monocytes activate STAT3 in neuroblastoma cells and alter their sensitivity to cytotoxic drugs (35, 44). Multiple mechanisms are associated with STAT3-mediated chemoresistance, including upregulation of the antiapoptotic protein survivin (45) or STAT3-mediated stimulation of DNA repair proteins (46, 47). Our study has identified that both of these antiapoptotic mechanisms are attenuated by targeted inhibition of STAT3 and thus may contribute to the enhanced chemosensitivity seen in our studies. The mechanisms by which STAT3 levels or its phosphorylation status affect DNA damage signaling responses (48, 49) are not well studied. Similar to our results, either etoposide or UV-induced DNA damage stimulated increased levels of P-ATR, P-ATM, and P-CHK1, which were attenuated when levels of STAT3 decreased (46, 47). In the UV-induced DNA damage model, increases in STAT3 levels were shown to directly stimulate increases in the steady-state levels of ATR (47). However, in this study as well as another (46), decreases or loss of STAT3 expression did not affect the steady-state levels of DNA damage response proteins. MDC1 is a key protein in the maintenance and amplification of DNA damage signals (49, 50). STAT3 was shown to regulate MDC1 promoter activity resulting in decreased MDC1 protein levels in $STAT3^{-/-}$ mouse embryonic fibroblasts (MEF) which may account for the decreases in DNA damage signaling and increased sensitivity to etoposide detected in $STAT3^{-/-}$ MEFs (46). Thus, STAT3 may influence the steady-state levels of proteins involved in the DNA damage sensing and amplifying pathways. A more detailed exploration of mechanisms mediating this increased sensitivity is planned for future studies.

In summary, this study assessed the effect of STAT3 inhibition in pediatric neuroblastoma models by 2 approaches: genetic inhibition using shSTAT3 or pharmacologic inhibition using as targeted ASO, AZD9150. This is the first assessment of the activity of AZD9150 in a pediatric cancer and has shown that AZD9150 inhibits total and activated STAT3 (P-STAT3) expression, increases chemosensitivity, and decreases tumorigenicity of neuroblastoma. These results suggest future clinical evaluation of selective STAT3 inhibition in combination with conventional cytotoxic therapy for patients with high-risk neuroblastoma.

Disclosure of Potential Conflicts of Interest

R. Woessner has ownership interest (including patents) in AstraZeneca Pharmaceuticals. No potential conflicts of interest were disclosed by the other authors.

Authors' Contributions

Conception and design: S. Yan, C.J. Thiele
Development of methodology: V. Veschi S. Yan, R. Woessner, C.J. Thiele
Acquisition of data (provided animals, acquired and managed patients, provided facilities, etc.): S. Odate, V. Veschi S. Yan, N. Lam
Analysis and interpretation of data (e.g., statistical analysis, biostatistics, computational analysis): S. Odate, V. Veschi S. Yan, N. Lam, C.J. Thiele
Writing, review, and/or revision of the manuscript: S. Odate, V. Veschi S. Yan, N. Lam, R. Woessner, C.J. Thiele
Administrative, technical, or material support (i.e., reporting or organizing data, constructing databases): S. Odate, N. Lam, R. Woessner, C.J. Thiele
Study supervision: N. Lam, C.J. Thiele

Acknowledgments

We would like to thank Dr. Zhihui Liu and members of the Cell & Molecular Biology Section, National Cancer Institute, for their thoughtful review of this study. We are grateful to AstraZeneca Pharmaceuticals, which provided AZD9150 and Ionis Pharmaceuticals, which kindly provided the ntASO. We appreciate the statistical expertise of Dr. David Venzon, Biostatistics of the Data Management Branch, CCR, NCI for advice on the limiting dilution analyses. This research was supported by the Center for Cancer Research, National Cancer Institute, NIH Intramural Research Program.

The costs of publication of this article were defrayed in part by the payment of page charges. This article must therefore be hereby marked *advertisement* in accordance with 18 U.S.C. Section 1734 solely to indicate this fact.

Received May 27, 2016; revised September 30, 2016; accepted October 4, 2016; published OnlineFirst October 19, 2016.

References

1. Brodeur GM, Pritchard J, Berthold F, Carlsen NL, Castel V, Castelberry RP, et al. Revisions of the international criteria for neuroblastoma diagnosis, staging, and response to treatment. J Clin Oncol 1993;11:1466–77.
2. Maris JM. Recent advances in neuroblastoma. N Engl J Med 2010;362:2202–11.
3. Maris JM, Hogarty MD, Bagatell R, Cohn SL. Neuroblastoma. Lancet 2007;369:2106–20.
4. Yu H, Pardoll D, Jove R. STATs in cancer inflammation and immunity: a leading role for STAT3. Nat Rev Cancer 2009;9:798–809.
5. Levy DE, Inghirami G. STAT3: a multifaceted oncogene. Proc Natl Acad Sci U S A 2006;103:10151–2.
6. Heim MH. The Jak-STAT pathway: cytokine signalling from the receptor to the nucleus. J Recept Signal Transduct Res 1999;19:75–120.
7. Aggarwal BB, Kunnumakkara AB, Harikumar KB, Gupta SR, Tharakan ST, Koca C, et al. Signal transducer and activator of transcription-3, inflammation, and cancer: how intimate is the relationship? Ann N Y Acad Sci 2009;1171:59–76.
8. Mullighan CG. JAK2–a new player in acute lymphoblastic leukaemia. Lancet 2008;372:1448–50.
9. Chen E, Staudt LM, Green AR. Janus kinase deregulation in leukemia and lymphoma. Immunity 2012;36:529–41.
10. Fiorini A, Farina G, Reddiconto G, Palladino M, Rossi E, Za T, et al. Screening of JAK2 V617F mutation in multiple myeloma. Leukemia 2006;20:1912–3.
11. Takemoto S, Ushijima K, Kawano K, Yamaguchi T, Terada A, Fujiyoshi N, et al. Expression of activated signal transducer and activator of transcription-3 predicts poor prognosis in cervical squamous-cell carcinoma. Br J Cancer 2009;101:967–72.
12. Garcia R, Bowman TL, Niu G, Yu H, Minton S, Muro-Cacho CA, et al. Constitutive activation of Stat3 by the Src and JAK tyrosine kinases participates in growth regulation of human breast carcinoma cells. Oncogene 2001;20:2499–513.
13. Xu YH, Lu S. A meta-analysis of STAT3 and phospho-STAT3 expression and survival of patients with non-small-cell lung cancer. Eur J Surg Oncol 2014;40:311–7.
14. Campbell CL, Jiang Z, Savarese DM, Savarese TM. Increased expression of the interleukin-11 receptor and evidence of STAT3 activation in prostate carcinoma. Am J Pathol 2001;158:25–32.
15. Mora LB, Buettner R, Seigne J, Diaz J, Ahmad N, Garcia R, et al. Constitutive activation of Stat3 in human prostate tumors and cell lines: direct inhibition of Stat3 signaling induces apoptosis of prostate cancer cells. Cancer Res 2002;62:6659–66.
16. Horiguchi A, Oya M, Shimada T, Uchida A, Marumo K, Murai M. Activation of signal transducer and activator of transcription 3 in renal cell carcinoma: a study of incidence and its association with pathological features and clinical outcome. J Urol 2002;168:762–5.
17. Monnien F, Zaki H, Borg C, Mougin C, Bosset JF, Mercier M, et al. Prognostic value of phosphorylated STAT3 in advanced rectal cancer: a study from 104 French patients included in the EORTC 22921 trial. J Clin Pathol 2010;63:873–8.
18. Ho PL, Kurtova A, Chan KS. Normal and neoplastic urothelial stem cells: getting to the root of the problem. Nat Rev Urol 2012;9:583–94.
19. Lin L, Liu A, Peng Z, Lin HJ, Li PK, Li C, et al. STAT3 is necessary for proliferation and survival in colon cancer-initiating cells. Cancer Res 2011;71:7226–37.
20. Ji J, Wang XW. Clinical implications of cancer stem cell biology in hepatocellular carcinoma. Semin Oncol 2012;39:461–72.
21. Sherry MM, Reeves A, Wu JK, Cochran BH. STAT3 is required for proliferation and maintenance of multipotency in glioblastoma stem cells. Stem Cells 2009;27:2383–92.
22. Ara T, Song L, Shimada H, Keshelava N, Russell HV, Metelitsa LS, et al. Interleukin-6 in the bone marrow microenvironment promotes the growth and survival of neuroblastoma cells. Cancer Res 2009;69:329–37.
23. Egler RA, Burlingame SM, Nuchtern JG, Russell HV. Interleukin-6 and soluble interleukin-6 receptor levels as markers of disease extent and prognosis in neuroblastoma. Clin Cancer Res 2008;14:7028–34.
24. Hsu DM, Agarwal S, Benham A, Coarfa C, Trahan DN, Chen Z, et al. G-CSF receptor positive neuroblastoma subpopulations are enriched in chemotherapy-resistant or relapsed tumors and are highly tumorigenic. Cancer Res 2013;73:4134–46.
25. Agarwal S, Lakoma A, Chen Z, Hicks J, Metelitsa LS, Kim ES, et al. G-CSF promotes neuroblastoma tumorigenicity and metastasis via STAT3-dependent cancer stem cell activation. Cancer Res 2015;75:2566–79.
26. Laverdiere C, Liu Q, Yasui Y, Nathan PC, Gurney JG, Stovall M, et al. Long-term outcomes in survivors of neuroblastoma: a report from the Childhood Cancer Survivor Study. J Natl Cancer Inst 2009;101:1131–40.
27. Yan S, Li Z, Thiele CJ. Inhibition of STAT3 with orally active JAK inhibitor, AZD1480, decreases tumor growth in Neuroblastoma and Pediatric Sarcomas In vitro and In vivo. Oncotarget 2013;4:433–45.
28. Hong D, Kurzrock R, Kim Y, Woessner R, Younes A, Nemunaitis J, et al. AZD9150, a next-generation antisense oligonucleotide inhibitor of STAT3 with early evidence of clinical activity in lymphoma and lung cancer. Sci Transl Med 2015;7:314ra185.
29. Li Z, Tan F, Liewehr DJ, Steinberg SM, Thiele CJ. In vitro and in vivo inhibition of neuroblastoma tumor cell growth by AKT inhibitor perifosine. J Natl Cancer Inst 2010;102:758–70.
30. Hu J, Lee H, Hermann A, Buettner R, Jove R. Revisiting STAT3 signaling in cancer: new and unexpected biological functions. Nat Rev Cancer 2015;14:736–46.
31. Regairaz MM, Munier F, Sartelet H, Castaing M, Mary V, Renauleaud C, et al. Mutation-independent activation of the anaplastic lymphoma kinase in neuroblastoma. Am J Pathol 2016;186:435–45.
32. Sattu K, Hochgrafe F, Wu J, Umapathy G, Schonherr C, Ruuth K, et al. Phosphoproteomic analysis of anaplastic lymphoma kinase(ALK) downstream signaling pathways identifies signal transducer and activator of

transcription 3 as a functional target of activated ALK in neuroblastoma cells. FEBS J 2013;280:5269–82.
33. Yadav A, Kalita A, Dhillon S, Banerjee K. JAK/STAT3 Pathway is involved in survival of neurons in response to Insulin-like growth factors and negatively regulated by suppressor of Cytokine signaling-3. J Biol Chem 2005;280:31830–40.
34. Chen B, Liang Y, He Z, An Y, Zhao W, Wu J. Autocrine activity of BDNF induced by the STAT3 signaling pathway caused prolonged TrkB activation and promoters human non-small cell lung cancer. Sci Rep 2016;6:30404.
35. Yang F, Jove V, Buettner R, Xin H, Wu J, Wang Y, et al. et al.Sorafenib inhibits endogenous and IL-6/S1P induced JAK2-STAT3 signaling in human neuroblastoma, associated with growth suppression and apoptosis. Can Biol Ther 2012;13:534–41.
36. Kroon P, Berry PA, Stower MJ, Rodrigues G, Mann VM, Simms M, et al. JAK-STAT blockade inhibits tumor initiation and clonogenic recovery of prostate cancer stem-like cells. Cancer Res 2013;73:5288–98.
37. Landier W, Knight K, Wong FL, Lee J, Thomas O, Kim H, et al. Ototoxicity in children with high-risk neuroblastoma: prevalence, risk factors, and concordance of grading scales–a report from the Children's Oncology Group. J Clin Oncol 2014;32:527–34.
38. Gariboldi MB, Ravizza R, Molteni R, Osella D, Gabano E, Monti E. Inhibition of Stat3 increases doxorubicin sensitivity in a human metastatic breast cancer cell line. Cancer Lett 2007;258:181–8.
39. Spitzner M, Roesler B, Bielfeld C, Emons G, Gaedcke J, Wolff HA, et al. STAT3 inhibition sensitizes colorectal cancer to chemoradiotherapy in vitro and in vivo. Int J Cancer 2014;134:997–1007.
40. Alas S, Bonavida B. Inhibition of constitutive STAT3 activity sensitizes resistant non-Hodgkin's lymphoma and multiple myeloma to chemotherapeutic drug-mediated apoptosis. Clin Cancer Res 2003;9:316–26.
41. Duan S, Tsai Y, Keng P, Chen Y, Lee SO, Chen Y. IL-6 signaling contributes to cisplatin resistance in non-small cell lung cancer via the up-regulation of anti-apoptotic and DNA repair associated molecules. Oncotarget 2015;6:27651–60.
42. Liu WH, Chen MT, Wang ML, Lee YY, Chiou GY, Chien CS, et al. Cisplatin-selected resistance is associated with increased motility and stem-like properties via activation of STAT3/Snail axis in atypical teratoid/rhabdoid tumor cells. Oncotarget 2015;6:1750–68.
43. Croucher JL, Iyer R, Li N, Molteni V, Loren J, Gordon WP, et al. TrkB inhibition by GNF-4256 slows growth and enhances chemotherapeutic efficacy in neuroblastoma xenografts. Cancer Chemother Pharmacol 2015;75:131–41.
44. Ara T, Nakata R, Sheard MA, Shimada H, Buettner R, Groshen SG, et al. Critical role of STAT3 in IL-6-mediated drug resistance in human neuroblastoma. Cancer Res 2013;73:3852–64.
45. Gritsko T, Williams A, Turkson J, Kaneko S, Bowman T, Huang M, et al. Persistent activation of stat3 signaling induces survivin gene expression and confers resistance to apoptosis in human breast cancer cells. Clin Cancer Res 2006;12:11–9.
46. Barry SP, Townsend PA, Knight RA, Scarabelli TM, Latchman DS, Stephanou A. STAT3 modulates the DNA damage response pathway. Int J Exp Pathol 2010;91:506–14.
47. Liao XH, Zhen L, He HP, Zheng DL, Wei ZQ, Wang N, et al. STAT3 regulated ATR via microRNA-383 to control DNA damage to affect apoptosis in A431 cells. Cell Signal 2015;27:2285–95.
48. Lowndes NF, Toh GW. DNA repair: the importance of phosphorylating histone H2AX. Curr Biol 2005;15:99–102.
49. Lou Z, Minter-Dykhouse K, Franco S, Gostissa M, Rivera MA, Celeste A, et al. MDC1 maintains genomic stability by participating in the amplification of ATM-dependent DNA damage signals. Mol Cell 2006;21:187–200.
50. Kastan MB, Lim DS. The many substrates and functions of ATM. Nat Rev Mol Cell Biol 2000;1:179–86.

Published OnlineFirst October 19, 2016; DOI: 10.1158/1078-0432.CCR-16-1317

Clinical Cancer Research

Inhibition of *STAT3* with the Generation 2.5 Antisense Oligonucleotide, AZD9150, Decreases Neuroblastoma Tumorigenicity and Increases Chemosensitivity

Seiichi Odate, Veronica Veschi, Shuang Yan, et al.

Clin Cancer Res 2017;23:1771-1784. Published OnlineFirst October 19, 2016.